Supporting Documents

Self-Healing of Glucose-Modified Polyurethane Networks Facilitated by Damage-Induced Primary Amines

Ying Yang and Marek W. Urban*
Department of Materials Science and Engineering
Center for Optical Materials Science and Engineering Technologies (COMSET)
Clemson University, Clemson, SC 29634
* - Corresponding author: mareku@clemson.edu

1. Mechanical Analysis

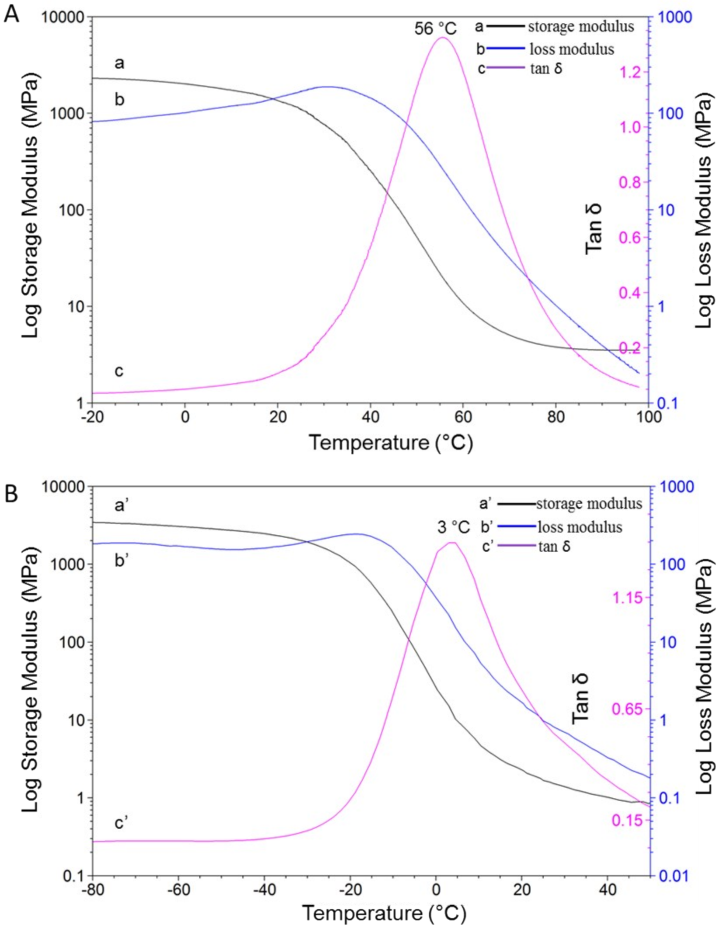

Figure S1. Storage modulus, loss modulus, and tan delta of MGP-PUR-Zn(OAc)$_2$ (Traces a, b, and c) and PUR-Zn(OAc)$_2$ (Traces a', b', and c') measured as a function of temperature using dynamic mechanical analysis (DMA).

Table S1. MGP/PEG ratios utilized to synthesize MGP-PUR-Zn(OAc)$_2$-a, MGP-PUR-Zn(OAc)$_2$-b, MGP-PUR-Zn(OAc)$_2$, and MGP-PUR-Zn(OAc)$_2$-c, their corresponding Young's moduli (G), and strain (ε)/stress (σ) before damage and after healing obtained from the stress-strain curves.

Specimen	MGP/PEG molar ratio	G (MPa)	ε after repair (%)	σ after repair (MPa)	ε before damage (%)	σ before damage (MPa)
MGP-PUR-Zn(OAc)$_2$-a	0.28/1	4.18	70.2	1.24	276	9.50
MGP-PUR-Zn(OAc)$_2$-b	0.44/1	29.6	82.9	5.03	289	13.3
MGP-PUR-Zn(OAc)$_2$	0.59/1	77.8	162	9.23	285	22.8
MGP-PUR-Zn(OAc)$_2$-c	0.73/1	344	4.00	4.49	298	35.5

2. Spectroscopic Analysis

Table S2. Tentative IR and Raman vibrational band assignments of MGP-PUR-Zn(OAc)$_2$ networks and their intensity changes (↓ or ↑) upon damage and repair. *

IR	Raman	Intensity changes upon damage	Intensity changes after repair	Tentative Assignments
Wavenumber (cm^{-1})				
	1756	↓	–	st C=O (HDI trimmer)
1710		↑	↓	st C=O (free urethane)
1680		↓	↓	st C=O (MGP-urethane, PEG-urethane and triisocyanate ring)
1633			↑	st C=O (urea)
1627		↑		st N-H (R-NH$_2$)
1562			↑	δ N-H (urea)
1527		↓	↓	δ N-H (urethane)
	1440	-	-	δ asymmetric C-H of hexane segments
	1328	↑	–	δ NC-H
	1305	↑	–	δ symmetric C-H of hexane segments
	1285	↑	-	δ OC-H
	1240	↑	-	
1270			↑	st C-N (urea)
1243		↓	↓	st C-N (urethane)
1150		↓	↓	st C-O-C (MGP-urethenas)
	1094	↓	–	C-C skeletal vibrations of hexane segments
1081		↑	↑	st C-OH (MGP) + δ C-O-C (urea)
	1067	↑	–	NC-C vibration
1045		↓	↓	st C-O-C (MGP-urethanes)
	1036	↓	-	OC-C vibration
1005		↑		st C-OH (MGP)

* G. Socrates, Infrared and Raman Characteristic Group Frequencies: tables and charts. John Wiley & Sons, 2004.

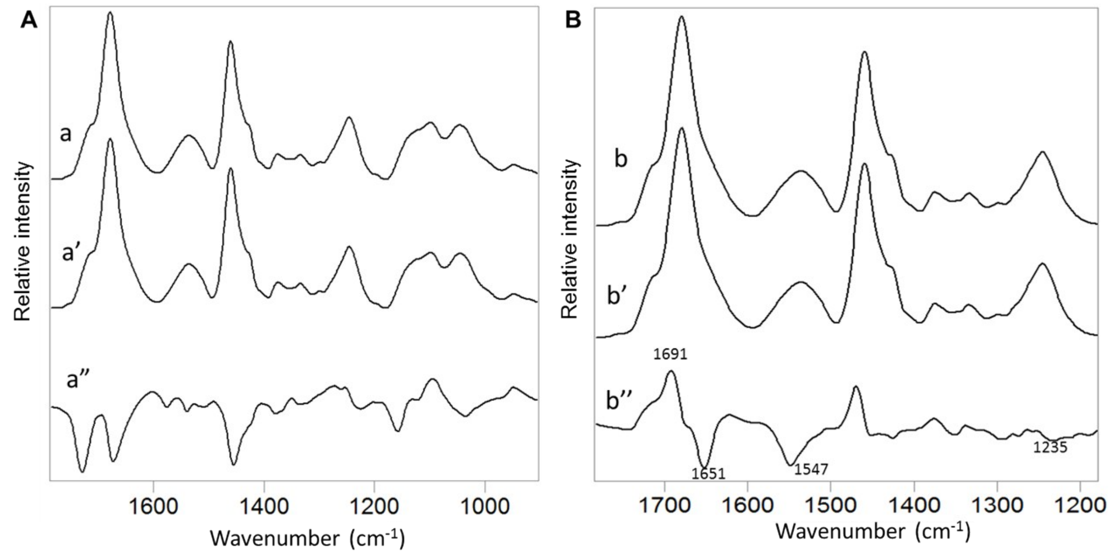

Figure S2. A - ATR-FTIR spectra of repaired (Trace a) and undamaged (Trace a') $Zn(OAc)_2$ catalyzed MGP-PUR after exposure to 40 °C for 7 days. Trace a" is the subtraction spectrum of Trace a-a'. B – ATR-FTIR spectra of repaired (Trace b) and undamaged (Trace b') $Zn(OAc)_2$ catalyzed PUR after exposure to 75 °C for 7 days. Trace b" is the subtraction spectrum of Trace b-b'.

3. Control Experiments and Data Analysis

The ability of $Zn(OAc)_2$ to catalyze MGP-PUR networks self-repair is predominantly determined by the susceptibility of urethane bonds toward nucleophiles, such as $–NH_2$ or –OH groups. In order to identify the reactivity of specific urethane linkages present in the MGP-PUR network, three control compounds were synthesized. They are shown in Scheme S1. Compound **MGP-4HI** was synthesized to represent the urethane linkages associated with MGP (MGP-urethane) in the network. Note, the urethane in C6 position of MGP has less steric hindrance compared to their counterparts in C2, C3, and C4 positions. Thus, C6 urethane is more stable, which was examined using compound **MGP-1HI**. **PEG-2HI** has the same structural elements as the urethane segments associated with PEG within MGP-PUR-$Zn(OAc)_2$ network.

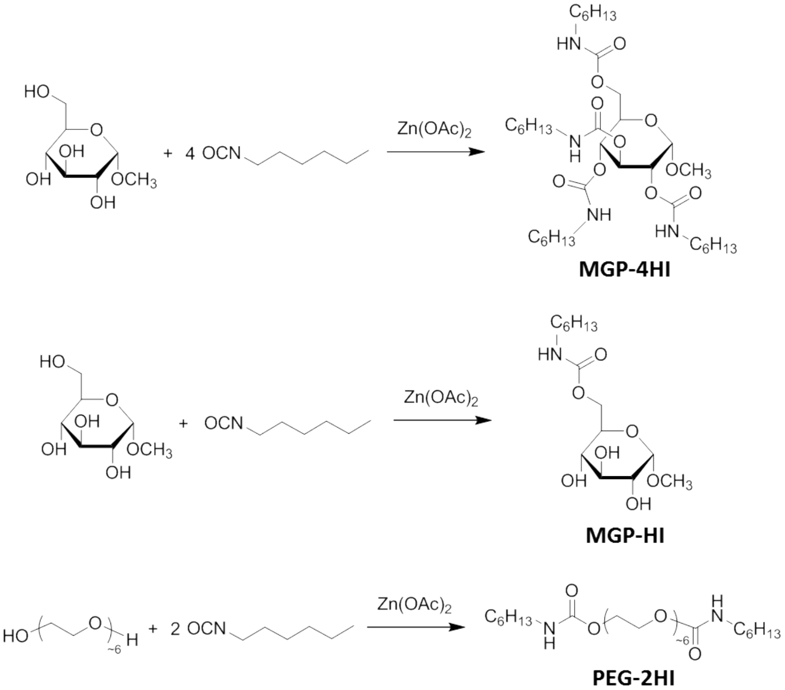

Scheme S1. Synthesis of control compounds **MGP-4HI, MGP-1HI,** and **PEG-2HI**.

To examine reactivity of **MGP-4HI** compound with nucleophiles, MGP-4HI was first reacted at 75 °C with a diamine compound, 2,2′-(Ethylenedioxy)bis(ethylamine) (EDBEA). ATR-FTIR spectra were recorded after 1, 5, 24, and 48 hrs of reaction to follow any change of the urethane bonds. The results are shown in Figure S3, A, which illustrate intensity decreases of the urethane bands at 1698 and 1550 cm^{-1} as well as new bands formation at 1620 and 1596 cm^{-1}. The 1620 cm^{-1} band is due to urea C=O vibrations, while the band at 1596 cm^{-1} is attributed to N-H vibrations of –NH_2. When the same reaction was carried out at 40 °C, only a small of amount urea was produced after 48 hrs of reaction, as manifested by the formation of a weak band at 1620 cm^{-1}. This is shown in Figure S3, B. When **MGP-4HI** was reacted with EDBEA without $Zn(OAc)_2$, no reaction occurred after 48 hr at 75 °C. This is shown in Figure S4, C, where the urethane bands at 1698 and 1550 cm^{-1} did not change intensities, and the formation of urea linkages was not observed. The reactivity of MGP-urethanes toward OH groups in the presence of $Zn(OAc)_2$ were also examined as shown in Figure S4, D. No reaction occurred within 48 hrs. Therefore, urethane bonds associated with MGP alone are thermally stable, but are able to react with –NH_2 when catalyzed by $Zn(OAc)_2$ at 75 °C, generating urea linkages.

Although 80% of the urethanes bonds of MGP-4HI are reacted with amine groups after 48 hrs, as shown in Figure S3, A, reactivity of the urethane in the C6 position of MGP is unclear. Thus, **MGP-1HI** was synthesized and reacted with EDBEA at 75 °C in the presence of 1.2% (w/w) $Zn(OAc)_2$. Decomposition of urethane linkages was observed, as shown in Figure S4, A, and manifested by the decrease of the 1698 cm^{-1} band. ATR-FTIR spectra of **PEG-2HI** reacted with EDBEA catalyzed by $Zn(OAc)_2$ at 75 °C is shown in Figure S4, B. No reaction has occurred. These results identified the reaction shown in Scheme S2 is responsible for formation of urea from reaction of –NH_2 with MGP-urethanes.

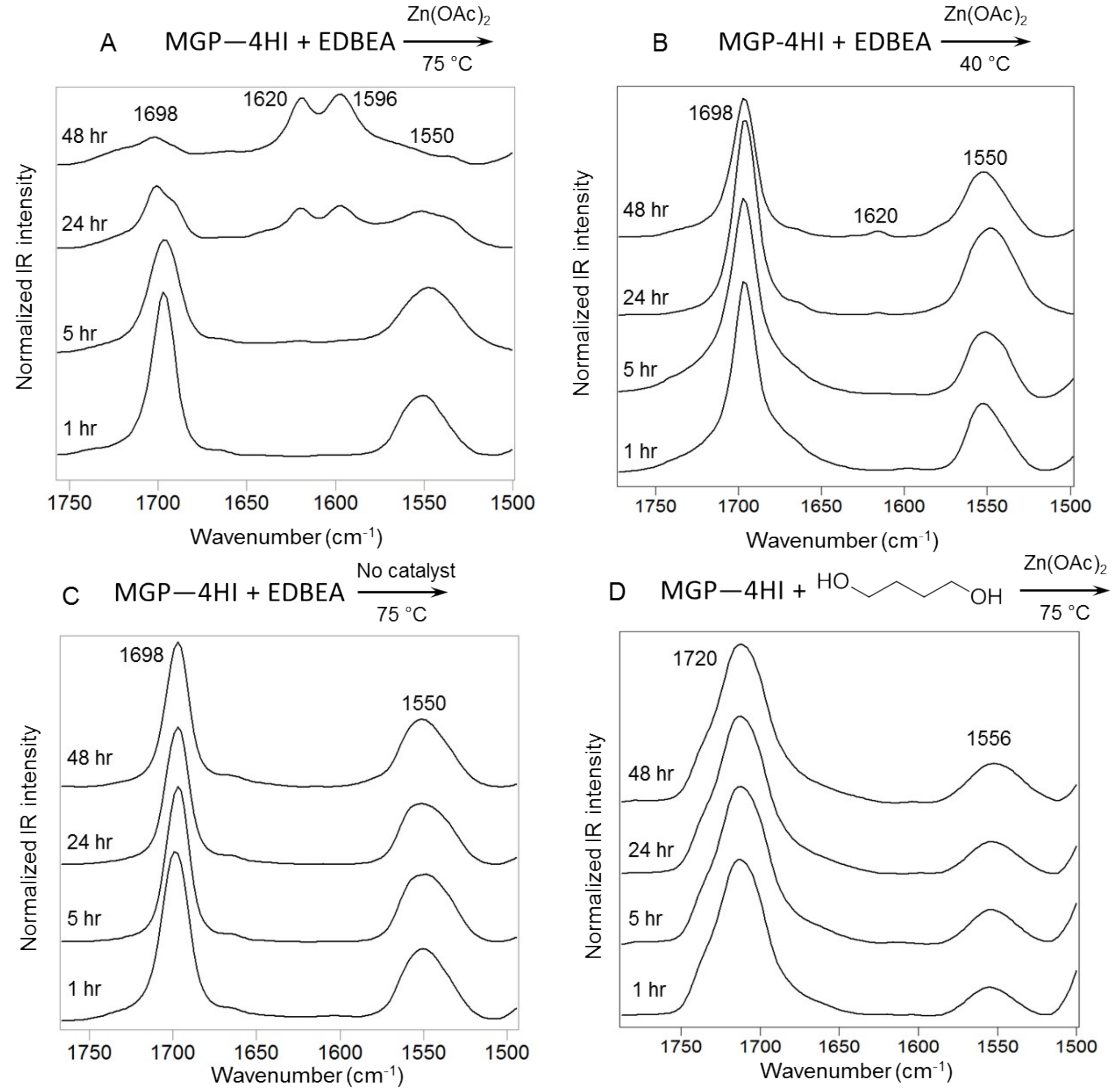

Figure S3. Figure A – D illustrates ATR-FTIR spectra of MGP-4HI reacted under the following conditions: A1 – MGP-4HI react with EDBEA catalyzed by $Zn(OAc)_2$ at 75 °C; A2 – MGP-4HI react with EDBEA catalyzed by $Zn(OAc)_2$ at 40 °C; A3 – MGP-4HI react with EDBEA at 75 °C without $Zn(OAc)_2$; A4 – MGP-4HI react with butanediol catalyzed by $Zn(OAc)_2$ at 75 °C. For each reaction, four ATR-FTIR spectra were collected after 1, 5, 24, and 48 hrs of reaction.

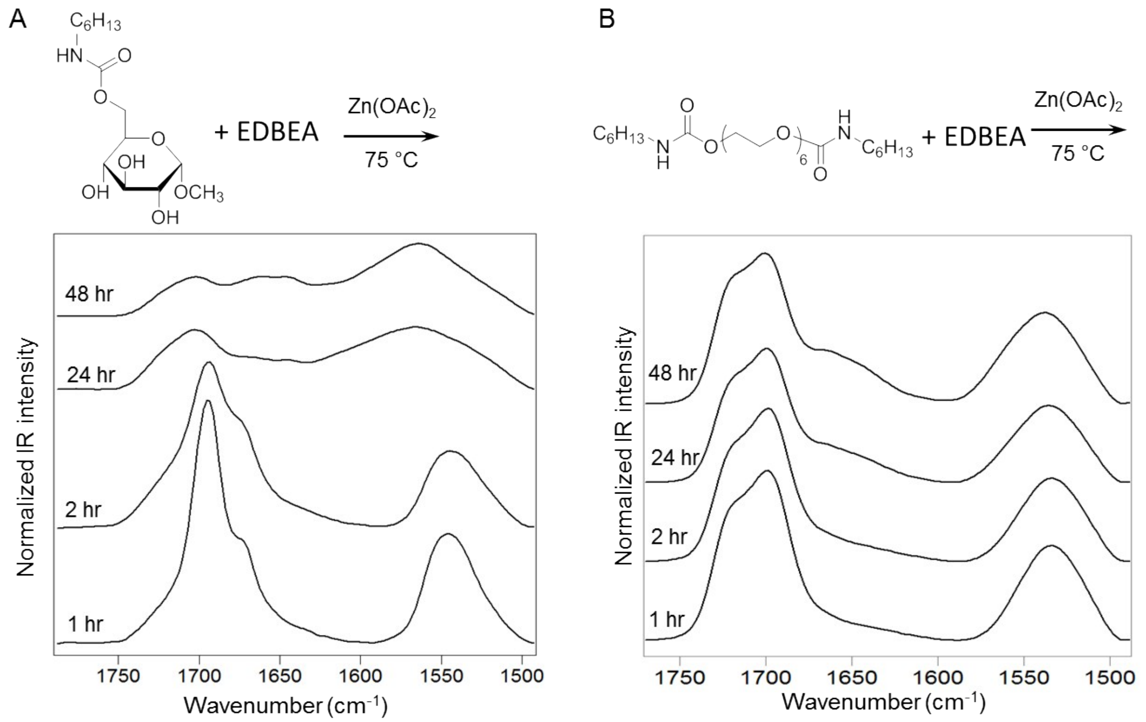

Figure S4. A – ATR-FTIR spectra of **MGP-1HI** reacted with EDBEA catalyzed by $Zn(OAc)_2$ at 75 °C; B - ATR-FTIR spectra of **PEG-2HI** reacted with EDBEA catalyzed by $Zn(OAc)_2$ at 75 °C. For each reaction, four spectra were collected after 1, 5, 24, and 48 hrs of reaction.

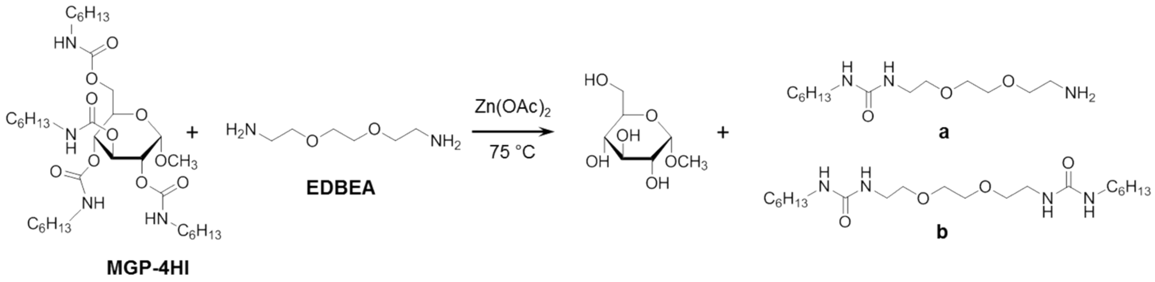

Scheme S2. Proposed reaction of the model compound MGP-4HI with EDBEA catalyzed by $Zn(OAc)_2$ at 75 °C.

In summary, the control experiments show that 80% of urethane bonds are reacted with amine groups and form urea linkages after 48 hrs. The reaction rates are significantly lower at 40 °C, where only a small amount of urea formation occurs after 48 hrs. However, no reaction occurs at 75 °C in the absence of $Zn(OAc)_2$ or EDBEA. Also, no reactivity of OH groups toward MGP-urethanes with the same amount of $Zn(OAc)_2$ at 75 °C was detected. Furthermore, PEG-urethane compounds synthesized by reacting PEG with two equivalent amounts of hexyl isocyanates are unreactive towards NH_2 functionalities under the same conditions, indicating higher stability of PEG-urethane linkages compared to MGP-urethanes.

4. Thermogravimetric Analysis (TGA)

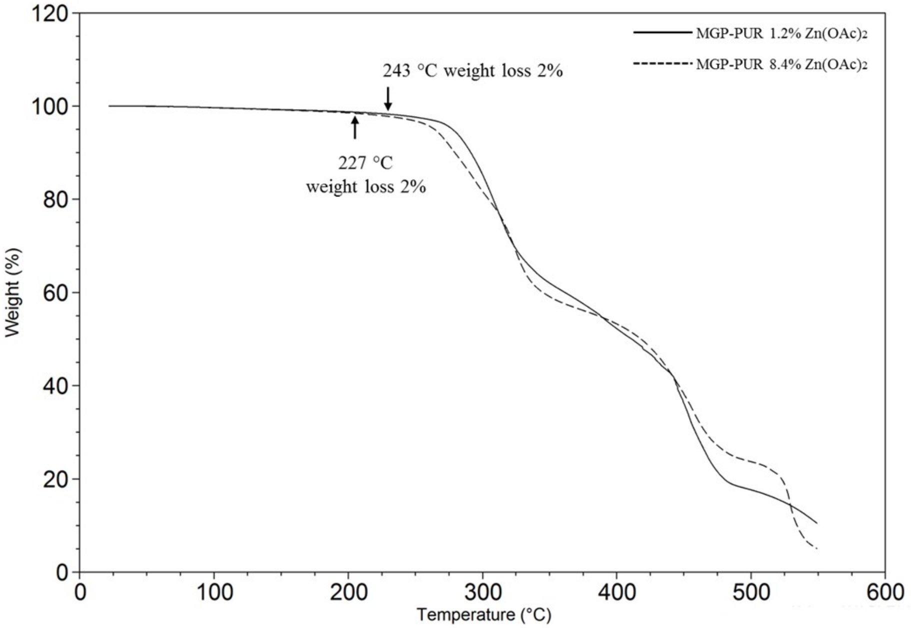

Figure S5. Thermogravimetric analysis (TGA) of MGP-PUR containing 1.2% (solid line) and 8.4% (dash line) of $Zn(OAc)_2$.

5. The Effect of Catalyst Concentrations

Concentrations of $Zn(OAc)_2$ in MGP-PUR were varied from 1.2 to 8.4% (w/w). As its concentration increased, self-healing efficiency decreased. This is shown in Table S3. The tensile stress after repair decreased significantly when concentration of $Zn(OAc)_2$ is increased from 1.2% to 3.6% (w/w). When $Zn(OAc)_2$ concentration levels are 8.4 % (w/w), MGP-PUR does not self-heal. When MGP-4HI is reacted with EDBEA, as the concentration of $Zn(OAc)_2$ increases from 0 to 8.4% (w/w), dissociation rate of MGP-urethane bonds at 75 °C increased, as shown in Figure S6. However, reaction kinetics in the solid state is different, and is dominated by diffusivity of reactants. The T_g of $Zn(OAc)_2$-catalyzed MGP-PUR films increases from 57.6 to 60.4 °C, as concentration of $Zn(OAc)_2$ increases from 1.2% to 8.4% (w/w). Their corresponding storage moduli at healing temperature (75 °C) increases from 3.9 to 6.9 MPa, while the loss modulus increases from 2.6 to 4.5 MPa. Although the T_g difference is only ~3 °C, slight variations in chain mobility at the repairing temperature due to Zn coordination is the determining factor responsible for self-repairing efficiency.

Table S3. MGP-PUR-$Zn(OAc)_2$ networks with various concentrations of $Zn(OAc)_2$ catalyst with their corresponding glass transition temperatures (T_g), storage (E') and loss (E") moduli at 75 °C, and tensile strain (ε)/stress (σ) after repairing at 75 °C for 7 days.

Specimen	Concentration of $Zn(OAc)_2$ (w/w%)	Tg (°C)	E' at 75°C (MPa)	E" at 75°C (MPa)	ε after repair (%)	σ after repair (MPa)
MGP-PUR-$Zn(OAc)_2$-1	0.2	59.6	2.54	1.98	80	2.9
MGP-PUR-$Zn(OAc)_2$	1.2	57.6	3.90	2.58	162	9.23
MGP-PUR-$Zn(OAc)_2$-2	3.6	58.3	5.31	3.28	3.4	1.48
MGP-PUR-$Zn(OAc)_2$-3	6	58.4	5.44	3.30	4.7	0.95
MGP-PUR-$Zn(OAc)_2$-4	8.4	60.4	6.9	4.56	0	0

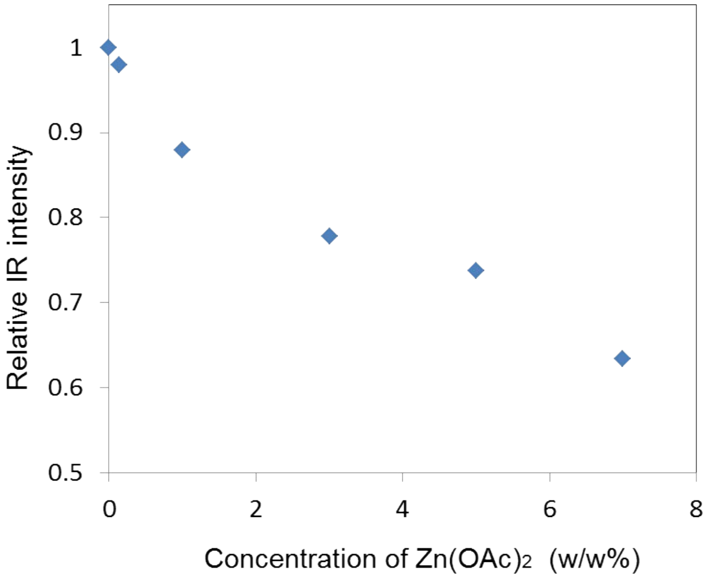

Figure S6. Relative IR intensity of urethane C=O vibrational band of MGP-4HI at 1698 cm^{-1} when MGP-4HI was reacted with EDBEA at 75 °C for 5 hrs plotted as a function of $Zn(OAc)_2$ concentrations.